MUSCLE SPINDLE FORCE SENSITIVITY IS CONSERVED IN THE PRESENCE OF INCREASED TENDON COMPLIANCE

A Dissertation
Presented to
The Academic Faculty

by

Jacob Stephens

In Partial Fulfillment
of the Requirements for the Degree
Master of Science in Biomedical Engineering in the
Wallace H. Coulter Department of Biomedical Engineering at Emory University and
Georgia Institute of Technology

Georgia Institute of Technology
August 2022

MUSCLE SPINDLE FORCE SENSITIVITY IS CONSERVED IN THE PRESENCE OF INCREASED TENDON COMPLIANCE

Approved by:

Dr. Lena Ting, Advisor
Wallace H. Coulter Department of Biomedical Engineering
Georgia Institute of Technology and Emory University

Dr. Young-Hui Chang
School of Biological Sciences
Georgia Institute of Technology

Dr. Gregory Sawicki
Woodruff School of Mechanical Engineering
Georgia Institute of Technology

Dr. Timothy Cope
School of Biological Sciences
Georgia Institute of Technology

Date Approved: May 4th, 2021

ACKNOWLEDGEMENTS

I would first like to thank my family for their continued support and encouragement, without which I would not be where I am now. I would also like to extend my thanks to my advisory committee for their continued guidance and advice. Additionally, thanks to Paul Nardelli, Dr. Emily Abbott, and Leo Wood for conducting and curating the experiments analyzed here. Finally, thanks to my colleagues at the Emory Neuromechanics Lab for their continual support.

TABLE OF CONTENTS

LIST OF TABLES

LIST OF FIGURES

LIST OF SYMBOLS AND ABBREVIATIONS

MTU	Musculotendon unit
IFR	Instantaneous firing rate
pps	Peaks per second
ASE	Added series elasticity
Fas	Fascicle
NC	Non-contractile
L	Length
v	Velocity
F	Force
Y	Yank
VAF	Variance accounted for

SUMMARY

Muscle spindles are complex sensory organs that relay vital mechanosensory information to the central nervous system to coordinate movement and control balance. However, the information that muscle spindles encode and the effects of muscle-tendon unit (MTU) mechanics on muscle spindle feedback are not well understood. Here, we applied sinusoidal length changes to the passive medial gastrocnemius of adult rats with and without added series elasticity to effectively increase tendon compliance. We measured the length change and force of the MTU, the length change of the muscle fascicle, and the resulting stretch responses of muscle spindles. We then compared various models of muscle spindle responses based on both MTU and fascicle-level mechanics to find the model that best describes muscle spindle behavior across a changing mechanical environment. We hypothesize that muscle spindles respond to the force and yank (the first time-derivative of force) exerted on muscle spindle fibers, and thus predict that muscle spindle responses will be best described by a model of the force and yank within the muscle fascicle. Our results demonstrate that while tendon compliance may affect muscle spindle behavior, muscle spindle responses are best described across mechanical conditions by force and yank models. Thus, any sensory loss due to increases in tendon compliance may be compensated for by increasing the forces exerted on muscle spindle fibers.

INTRODUCTION

1.1 Structure and Function of Muscle Spindles

Muscle spindles are complex mechanosensory organs that lie embedded in muscles and relay information regarding muscle stretch to the central nervous system via group Ia sensory afferents. These sensory afferents form direct connections with motor neurons in the spinal cord (the stretch reflex loop), but also relay information along channels in ascending pathways in the spinal cord and up to the brain [1, 2]. With a combination of both peripheral and central pathways, muscle spindles play a vital role in the neural control of movement [3]. Lockhart and Ting [4] demonstrated that during balance perturbations in cats, a large burst of activity in antagonist muscles was present shortly after the onset of the perturbation, and that this response was absent in cats with sensory neuropathy. It's also been demonstrated that these sensory-driven muscular responses are directionally-tuned in healthy cats, implying a relationship to muscle stretch [5, 6]. Additionally, disruption of these sensory pathways disrupts inter-joint coordination in cats, particularly during down-hill walking [7]. A genetic strain of mice without muscle spindles have also been shown to have decreased speed, altered muscle activity, and reduced ability to respond to perturbations during locomotion [2, 8]. The same genetic strain of mice also has a marked lack of joint coordination during swimming, when more fine control is required, and decreased foot placement accuracy during ladder walking [2]. It's also been shown in amputees that the loss of sensory feedback from muscle spindles and Golgi tendon organs

results in a loss of sensorimotor activity in the brain and increased compensation with the visual system to coordinate movement [9].

Though muscle spindles play a key role in the control of movement, a clear understanding of their behavior and information they encode remains elusive. Muscle spindles are small organs that lie embedded in the parent muscle, however previous descriptions of their behavior have largely relied on measurements of joint-level mechanics or the mechanics of the musculotendon unit (MTU). As the muscle and tendon are arranged in series, and their stiffness can differ, the length change of muscle fascicles (bundles of muscle fibers) may be substantially different from the length change of the MTU [10].

1.2 Force- and Length-Sensing Behaviors of Muscle Spindles

Recent evidence suggests that muscle spindles may be sensitive to force and yank (the first time-derivative of force, dF/dt) rather than length or velocity [11-13]. Muscle spindle responses have been shown to be related to muscle stretch length but are particularly sensitive at shorter stretches [14]. Additionally, the peak firing rates of muscle spindles have been shown to be nonlinearly related to stretch velocity in ramp-and-hold stretch paradigms [15]. This same mathematical relationship to stretch velocity has also been shown to reproduce spindle firing rates over time during active locomotion cycles in cats [16]. Additionally, *in vivo* muscle spindle firing rates in humans has been shown to be closely related to muscle fascicle length during slow sinusoidal stretches of the soleus [17]. These examples from a large body of work contributed to the understanding of muscle spindles as length and velocity sensors in the muscle.

However, muscle spindle firing responses have been shown to exhibit the same thixotropic properties as muscle, and models of crossbridge binding have been shown to reproduce key qualitative features of muscle spindle behavior [11, 18-23]. This is hypothesized to be due to the force-producing properties of intrafusal muscle fibers, or the muscle fibers within the spindle that attach to sensory encoding regions within spindle fibers. Further, in passive cat muscles (with an absence of alpha motoneuron drive to extrafusal muscle and gamma motoneuron drive to intrafusal muscle), muscle spindle responses have been accurately reproduced by linear combinations of force and yank measured from the MTU [12]. Thus, in the absence of central drive, extrafusal muscle and muscle spindle stretch responses appear to be governed by the same force-producing properties. However, MTU force and yank are not the most accurate predictors of spindle firing in rats. Due to dense extramysial tissue within rat muscle, MTU force and yank fail to accurately reproduce spindle firing at longer stretch lengths. However, subtracting the estimated force contribution of these non-contractile tissues from the force of the MTU corrects this discrepancy [13].

1.3 Effect of Tendon Stiffness

Tendon stiffness disrupts the relationship between the forces and length changes of the tissue surrounding the muscle spindle from the mechanics of the joint. As muscle fascicles and tendons are arranged in series, the length change of the fascicles with respect to the length change of the MTU is determined by tendon stiffness, as shown in Fig. 1. Furthermore, tendons can disrupt the relationship between the force in contractile muscle tissue and the force in the tendon. While arranged in series, the dense connective tissue in rats results in a change in force distribution between contractile and non-contractile

muscular tissues that depends on fascicle length. Given the exponential force-length relationship of non-contractile tissue [13], at longer fascicle lengths this tissue accounts for a greater proportion of the total MTU force. Thus, changes in tendon stiffness can directly decouple the relationship between MTU and fascicle length, and indirectly decouple the relationship between MTU and fascicle force.

1.4 Clinical Significance

While direct recording from muscle spindle afferents is possible in awake humans, current techniques severely limit the possible behaviors in which spindle afferent activity can be measured. For this reason, robust, generalizable, and predictive models are required to understand the role of muscle spindle feedback in human movement and balance control. A generalizable model of muscle spindle behavior should be accurate regardless of the mechanical properties of the MTU. For example, aging, exercise, and certain conditions can change the mechanical properties of both the muscle and tendon [24, 25], and a generalizable muscle spindle model should be accurate in all such cases. In addition, models of increased sensory feedback based on force have reproduced key features of gait and clinical tests of spasticity in children with cerebral palsy [26, 27]. To develop such a generalizable model, it is important to consider the lengths and forces of the tissue neighboring the muscle spindle rather than using MTU- or joint-level approximations. As tendon stiffness affects the relationships between MTU and fascicle forces and length changes, muscle spindle models based on fascicle-level mechanics will serve to offer greater insight into what information is relayed by muscle spindles to the central nervous system and allow for generalizable descriptions of spindle behavior.

1.5 Hypothesis

Here, we set out to test the force sensitivity of muscle spindles in altered mechanical conditions by measuring muscle spindle afferent firing rates in response to imposed sinusoidal stretches (2 mm amplitude at 2 Hz) of the medial gastrocnemius (MG) musculotendon unit (MTU) with and without added series elasticity (ASE). The MG was in a passive state in the portions of trials analyzed here, such that there was no descending drive to the muscle or muscle spindles. We hypothesize that muscle spindles respond to the force and yank exerted on intrafusal muscle fibers. According to this hypothesis, the reduction in stiffness of the MTU will result in a decrease in force within the muscle itself, and thus firing rate will decrease. Due to the redistribution of force between contractile and non-contractile tissues in the muscle, we predict that a mathematical model of spindle firing based on fascicle force and yank will better predict spindle IFR across experimental conditions than one based on MTU force and yank, assuming fascicle force is approximately proportional to intrafusal force. According to previous descriptions of muscle spindle responses with respect to the length change and velocity of the MTU, we also considered models of spindle behavior based on the length change and velocity of the MTU and fascicle. As the imposed sinusoidal stretches are similar to muscle stretch patterns during locomotion in rats, we also considered the nonlinear velocity model formulated by Prochazka and Gorassini [15]. We predict that these models will reasonably predict muscle spindle firing rates when trained in the control condition, but their accuracy will decrease in the ASE condition.

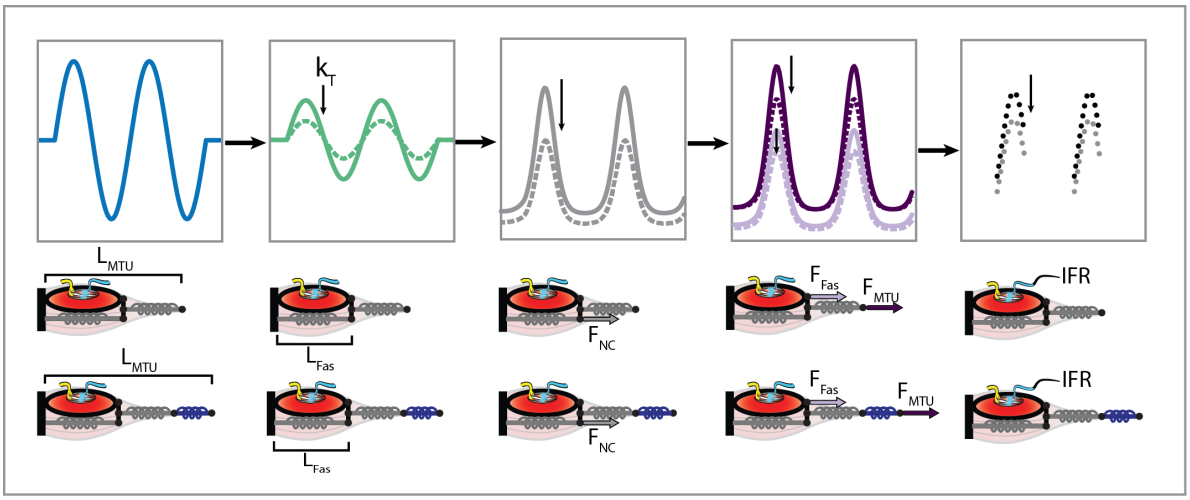

Figure 1: Predicted decoupling of MTU and fascicle lengths and forces with an increase in tendon compliance. For the same given displacement of the MTU, increased tendon compliance will decrease the strain of the fascicle. This in turn reduces the force contribution of extramysial tissue, which changes the distribution of MTU force between contractile and non-contractile tissues. The reduced force within the muscle will hypothetically result in a decrease in firing rates of a spindle within the fascicle.

METHODS

2.1 Animal Preparation

All animal procedures were conducted according to guidelines of the Georgia Institute of Technology Institutional Animal Care and Use Committee. Adult female Wistar rats (250 – 300g body weight) were deeply anesthetized by isoflurane inhalation until the withdrawal reflex was absent. Temperature, respiratory rate, heart rate, PCO2, and SPO2 were continuously monitored for the duration of each experiment. Animals were euthanized by isoflurane overdose and exsanguination.

Animal dissection was conducted in the same manner described in Vincent et al 2017 [1]. The medial gastrocnemius (MG) was dissected away from the other muscles of the triceps surae and cut away from the calcaneus. The MG tendon was fixed to the arm of a servomotor (AURORA 310C-LR). In the control condition, the tendon was fixed using Kevlar thread. In the ASE condition, the tendon was tethered to a piece of surgical tubing, which was in turn fixed to the motor. Sonomicrometry crystals (Sonometrics) were implanted at the proximal and distal ends of the same fascicle within the MG. The MG nerve was isolated from surrounding tissues and other nerves were crushed. Dorsal roots of the L4 and L5 were dissected and suspended on a bipolar hook electrode for recording. Alpha motoneurons were also stimulated to elicit contraction of extrafusal MG muscle fibers, however for the purposes of this analysis only passive cycles of these trials were examined.

2.2 Data Collection

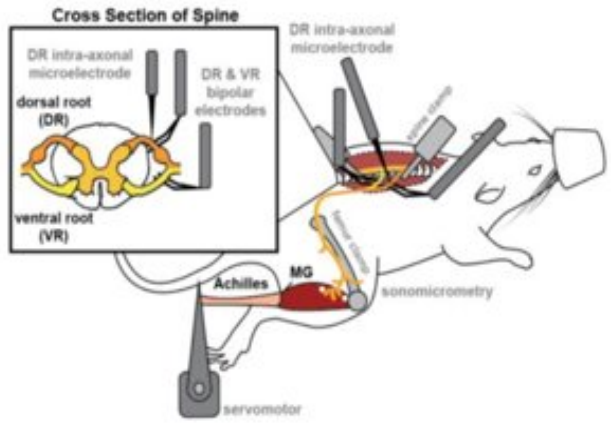

Figure 2: Experimental design. Length change and force of the MG MTU was controlled via servomotor and length change of the MG fascicle was measured via sonomicrometry. Resulting spindle afferent action potentials were recorded from the dorsal root of the spinal cord and stimulating electrodes were placed on the ventral roots, although only passive cycles of trials are not considered here.

Recordings from spindle afferents (n = 12) from 5 animals were taken intracellularly via glass microelectrode. MTU length and force were measured from the servomotor, and muscle fascicle length was measured with sonomicrometry at 20 kHz (Fig. 2). Data was collected and stored using Cambridge Electronic Design (CED) Power 1401 and Spike2 software.

2.3 Data Processing

For each trial, MTU and fascicle displacements were first normalized such that the resting length was 0. Force measurements were low-pass filtered at 1 kHz with a 2^{nd}-order Butterworth filter. Measurements were then downsampled to approximately 3.5 kHz. MTU length, fascicle length, and force were then all filtered using a 1^{st}-order Savitzky-Golay filter with a window of 501 samples. Then, a 6^{th}-order Savitzky-Golay filter with a window size of 151 samples (approximately 43 ms) was used to smooth length and force measurements and differentiate to obtain velocity and yank measurements. Trials were

excluded on the basis of having no recorded spikes or of having unreliable force measurements, in which rapid changes in force were observed at the peak of the stretch cycle with no accompanying changes in MTU or fascicle length, indicating potential slipping of the MTU on the motor.

2.4 Computational Modeling

All computational modeling was generated in MATLAB software (The MathWorks, Inc.) using constrained optimization. A total of six models were compared. The first tested the relationship between the force and yank of the MTU measured from the motor, given in Equation 1. The second utilized the estimated force and yank on the contractile tissue of the muscle, termed "fascicle" force and yank, given by Equation 2. These fascicle force and yank models are similar to those given by Blum et al 2019 [13], with the noted change of utilizing the length of the fascicle as opposed to the length of the MTU to estimate the force and yank on non-contractile tissues, and are given by Equations 3 and 4. The third (Equation 5) and fourth (Equation 6) utilized the length and velocity of the MTU measured from the motor, and the length and velocity of the fascicle measured with sonomicrometry, respectively. The fifth and sixth (Equations 7 and 8, respectively) utilized the velocity of the MTU and velocity of the fascicle, fitted with a fractional power law model similar to Prochazka and Gorassini 1998 [16].

$$\widehat{IFR}(t-\lambda) = k_F(F_{MTU} + b_F) + k_Y Y_{MTU} \quad (1)$$

$$\widehat{IFR}(t-\lambda) = k_F(F_{Fas} + b_F) + k_Y Y_{Fas} \quad (2)$$

$$F_{Fas} = F_{MTU} - F_{NC} = F_{MTU} - \left(Ae^{k_{exp}(L_{Fas}-L_0)} + k_{lin}\left(L_{\{Fas)} - L_0\right)\right) \quad (3)$$

$$Y_{Fas} = Y_{MTU} - Y_{Fas} = Y_{MTU} - \left(Ak_{exp}e^{k_{exp}(L_{Fas}-L_0)}v_{Fas} + k_{lin}v_{Fas}\right) \quad (4)$$

$$\widehat{IFR}(t-\lambda) = k_L(L_{MTU} + b_L) + k_V v_{MTU} \quad (5)$$

$$\widehat{IFR}(t-\lambda) = k_L(L_{Fas} + b_L) + k_V v_{Fas} \quad (6)$$

$$\widehat{IFR}(t-\lambda) = k_V v_{MTU}^{k_P} + b_V \quad (7)$$

$$\widehat{IFR}(t-\lambda) = k_V v_{Fas}^{k_P} + b_V \quad (8)$$

These models were implemented in algorithms to optimize coefficients to fit model predictions to IFR using minimization of sum of squares error. Ranges for each coefficient could be specified, and the algorithm would determine coefficients within those ranges that minimized the error. Limits for gains (k_F, k_Y, k_L, and k_V) were loosely restrained, such that upper limits on the coefficients did not force the fitting in any particular direction. However, non-zero lower limits were set for k_F and k_L to ensure some contribution from each component to the model fit. The limits for the power law models were set in a manner as to align with the values specified in Prochazka and Gorassini 1998 [16]. The reported value for k_V was 4.3, so the limit was set between 1 and 20, the value for k_P was 0.6, and limits were set between 0.1 and 2, and the value for b_V was 82, so the limits were set at 40 and 120. The ranges for these values were expanded slightly to account for differences in

scale of MTU and fascicle velocity. The ranges for the time delay lambda were set between 0 and 20 ms.

Ranges and constraints for non-contractile coefficients were set in a manner that agreed with Blum et al 2019 [13] and to be physiologically plausible. Constraints were set to ensure the estimated fascicle force was in tension when spiking occurred (allowing slack during shortening phases), the fascicle was in tension at rest, and the non-contractile force accounted for between 20 and 40 percent of the total MTU force (reported to be 34.3% for 2 mm stretches in Blum et al 2019 [13]) and 10 and 80% of MTU yank. Ranges for coefficients were specified such that A was between 0 and 2.0 N, k_{exp} was between 0.5 and 3.0 mm^{-1}, L_0 was between 0 and 0.25 mm, and k_{lin} was between 0 and 1.0 N/mm.

Each model fit was conducted on an individual trial basis, and certain coefficients were then prescribed as needed. First, the time delay was assumed to be consistent for each afferent, so after fitting each trial, optimal values were determined for each afferent, then set as constants for further iterations of fitting. Each animal was assumed to have the same non-contractile tissue properties, so after individually fitting, optimal coefficients were determined for each animal and set as constants in the next iteration of fitting. Non-contractile coefficients were fixed once per fitting iteration in order to ensure that the next iteration of fitting would still meet the constraints. Optimal values for non-contractile coefficients were determined by taking the maximum likelihood estimator of individual trial fit values to reduce the effect of potential outlier fits. Optimal values for lambda were determined by weighted average, where the weight was the R-squared value of the model fit, such that values that led to a better fit were given preference.

To determine the cross-predictive accuracy of each model, an optimal set of coefficients was determined for each afferent. Assuming one spindle had the same "sensitivities" in each model, a single set of coefficients was used to predict spindle afferent firing rates in both control and ASE conditions. Optimal coefficients were determined in the same way as lambda previously, by taking a weighted average of values with individual fit R-squared serving as the weight. Only values from the control condition were used in determining these optimal coefficients, in order to assess how these model predictions generalized to the ASE condition.

2.5 Data Analysis

Model accuracy was assessed using R^2 and variance accounted for (VAF) metrics. R^2 was computed as the square of Pearson's correlation coefficient, given by Equation 9.

$$\mathrm{P}\left(IFR, \widehat{IFR}\right) = \frac{1}{N-1}\sum_{i=1}^{N}\left(\frac{IFR_i - \mu_{IFR}}{\sigma_{IFR}}\right)\left(\frac{\widehat{IFR_i} - \mu_{\widehat{IFR}}}{\sigma_{\widehat{IFR}}}\right) \tag{9}$$

$$VAF = 1 - \frac{var\left(IFR - \widehat{IFR}\right)}{var(IFR)} \tag{10}$$

In this case, IFR_i represents recorded muscle spindle IFR and $\widehat{IFR_i}$ represents the predicted firing rate at each instance *I* over *N* samples. The correlation coefficient ρ was computed using MATLAB's built-in *corrcoef()* functionality. Similarly, VAF was computed using the variance of the residual errors and of the recorded IFR according to Equation 10 [28, 29].

Once performance metrics had been computed, they were collected and exported for statistical analysis with R software (The R Foundation). To compare the predictive accuracy of models in control and ASE conditions, the R^2 and VAF of individual-trial fits and fixed-coefficient fits were compared. Statistical comparisons were made using the accuracy (R^2 or VAF) as the outcome, with ASE as a fixed effect and individual afferents as a random effect. Thus, statistical comparisons assessed the change in performance of each model per afferent with the addition of elasticity. Next, to assess any change in accuracy associated with model training, individual-trial fit accuracy was compared to the fixed-coefficient fit accuracy in the control condition using a paired t-test.

RESULTS

3.1 Decoupling of MTU and Fascicle Lengths and Forces with ASE

As predicted, the addition of series elastic elements altered the relationships between the lengths and forces of the MTU and fascicle. For the same imposed length change of the MTU, the length change of the fascicle decreased, the force of the MTU decreased, and spindle afferent firing rates decreased. Increased tendon compliance decreased fascicle stretch the most at longer lengths. The addition of tendon compliance decreased force and fascicle excursion, however had no effect on the apparent stiffness of the muscle with respect to fascicle length, as demonstrated by the relationships between MTU and

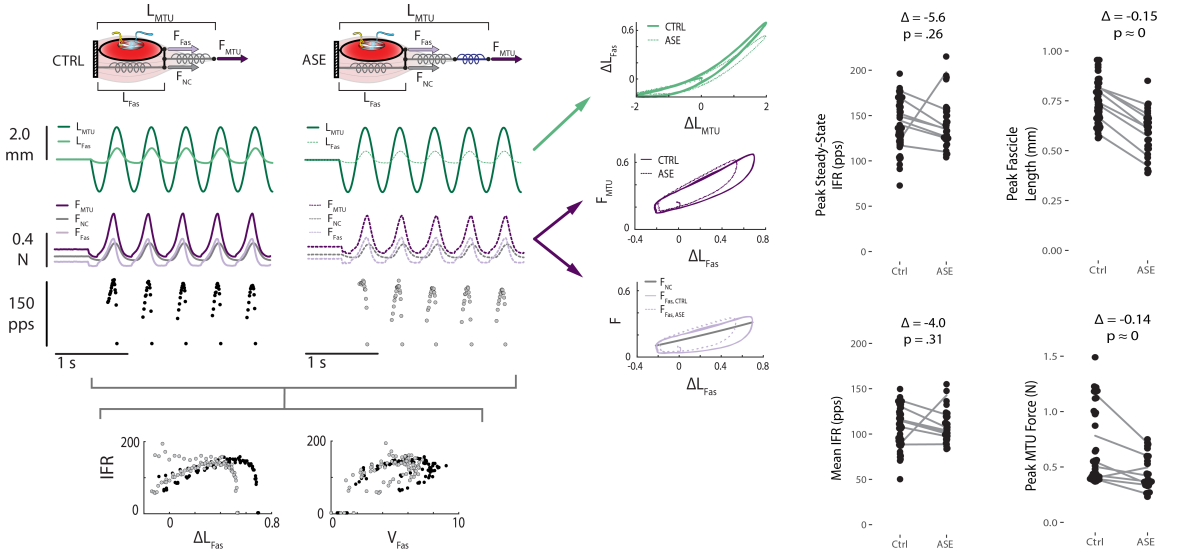

Figure 3: Decoupling of MTU and fascicle dynamics and relationships to muscle spindle IFR. Increases in effective tendon compliance did not significantly reduce mean or peak steady-state firing rate but did result in decreases in MTU force and fascicle length. While increased compliance decreased peak MTU force, it did not change the apparent stiffness of the MTU with respect to fascicle length. Increased compliance also altered the relationship between fascicle length and velocity and muscle spindle IFR, with firing rates decreasing at lower stretch lengths and velocities.

estimated fascicle force with respect to fascicle length. Fig. 3 shows the relationships between spindle firing rate, and measured fascicle length and velocity. Length and velocity relationships demonstrate similar relationships with the addition of compliance, with firing rates dropping off more quickly with ASE.

3.2 Force and Yank Model

To test the hypothesis that muscle spindles respond to the force and yank exerted on intrafusal muscle fibers, we compared predictive models of muscle spindle afferent firing rates with and without ASE. Figure 4 demonstrates examples of the force and yank fitting models. Fig 4a shows examples of MTU and fascicle force and yank models. Both models have been tested previously [12, 13], however this present analysis offers direct comparisons of the predictive accuracy of the two. The comparison of recorded vs predicted IFR in the MTU force and yank model shows accurate predictions at high firing rates, however it tends to under- or over-predict in the mid-range, a consistent trend across trials. Comparisons of recorded vs predicted IFR in the fascicle force and yank model show less tendency to under- and over-predict in the intermediate range of firing rates.

Comparisons of cross-prediction accuracy (fixed-coefficient fits) in Fig 4b indicated similar trends in fitting as in the individual fits regarding under- and over-predicting intermediate firing rates. Slight differences in the relationship between recorded and predicted IFR can be observed in the MTU model, while the fascicle model produced more consistent relationships. In the curves shown, the models with fixed coefficients under-

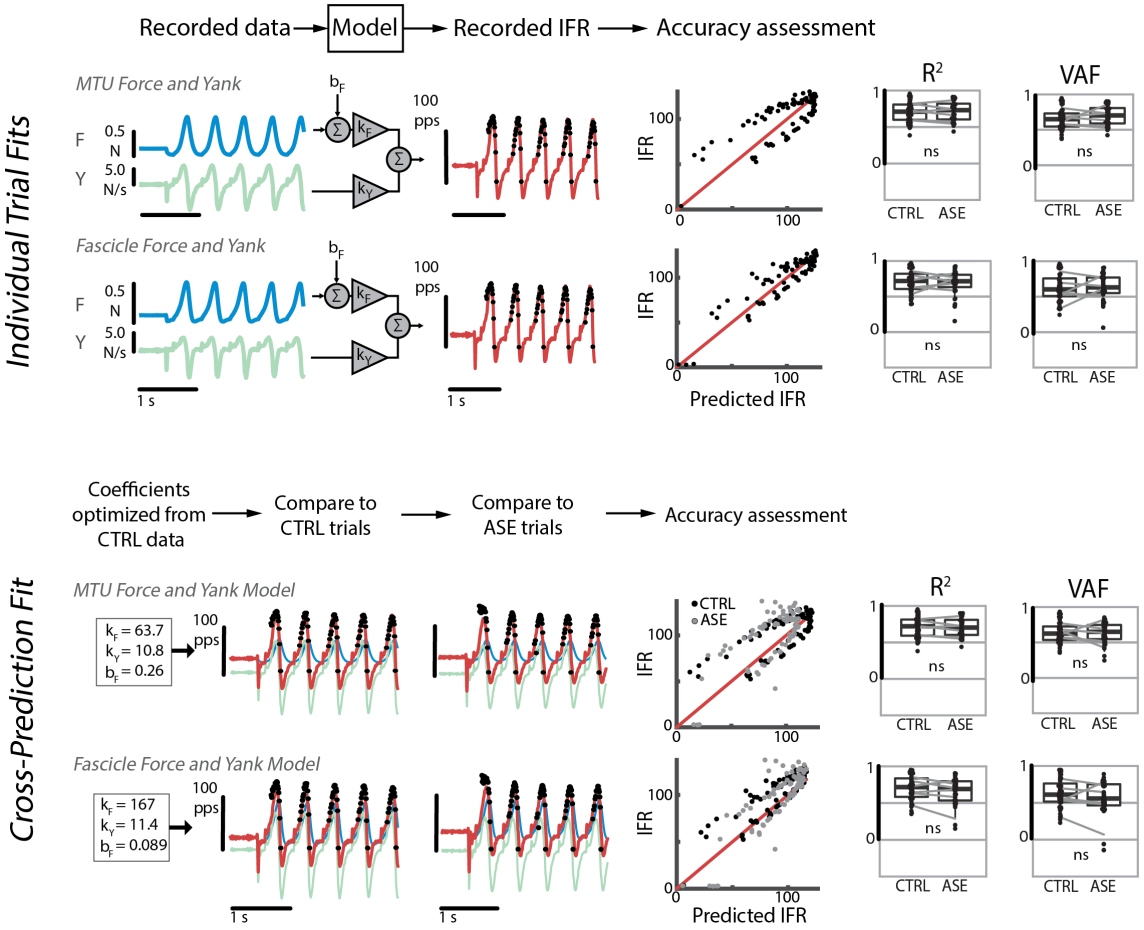

Figure 4: Predictions of muscle spindle IFR based on MTU and fascicle force and yank. Top panel: Example individual-trial fits of MTU and fascicle models. Force (blue) and yank (green) are combined in a pseudo-linear manner to fit the firing rate profile (red) of the muscle spindle afferent. Comparison of recorded and predicted IFR (right, red line indicating a 1:1 relationship). No significant differences in R^2 or VAF were observed between conditions for either model. Bottom panel: optimized coefficients for each afferent (trained on control condition trials) were used to predict firing rates across conditions. MTU model shows a slight shift towards under-prediction in the ASE condition, however no significant loss of accuracy was observed in either model.

predict firing rate during the stretch phase and over-predict during shortening. Altogether, the MTU force and yank model prediction accuracy was not significantly affected by tendon compliance. Comparing individual trial fits revealed no significant change in R^2 or VAF between conditions. Similarly, no significant change was present in R^2 or VAF

between groups in fixed-coefficient fits. Fixed-coefficient R^2 was slightly but significantly greater than single-trial fit R^2 in the control condition, however no significant relationship was found in VAF.

Similarly, added tendon compliance had no effect on the accuracy of the fascicle force and yank model. R^2 and VAF were consistent for individual trial fits across conditions, and no significant changes were present across groups for fixed-coefficient fits as well. There was also no significant difference in R^2 or VAF from individual-trial fits to fixed-coefficient fits.

3.3 Length and Velocity Model

Considering the alternative hypothesis that muscle spindles respond to stretch length and velocity, we compared predictions of muscle spindle firing modeled by linear combinations of both MTU and fascicle displacement and velocity. To test the generalizability of these models across mechanical conditions, a single set of coefficients was determined based on fit coefficients in the control condition and used to predict IFR for the same afferent in the ASE condition. Fig. 5 shows model predictions of spindle firing rate based on the length and velocity of the MTU and fascicle. In the individual-trial fits in Fig. 5, both models predict intermediate firing rates with less accuracy than the force and yank models, and the relationship between recorded and predicted IFR is increasingly nonlinear. Further, this issue is not substantially improved by utilizing fascicle measurements. Fixed- coefficient fits of both MTU and fascicle models show no change in the nonlinear relationship of recorded vs predicted IFR. However, in the MTU model, the firing rates of the model fit are consistent between control and ASE conditions, while in

the fascicle model, the relationship between recorded and predicted IFR changes between conditions. In the MTU length and velocity model, no significant changes in R^2 or VAF were observed in individual fits between control and ASE conditions. In fixed-coefficient fits, no significant change was observed in the R^2 between control and ASE

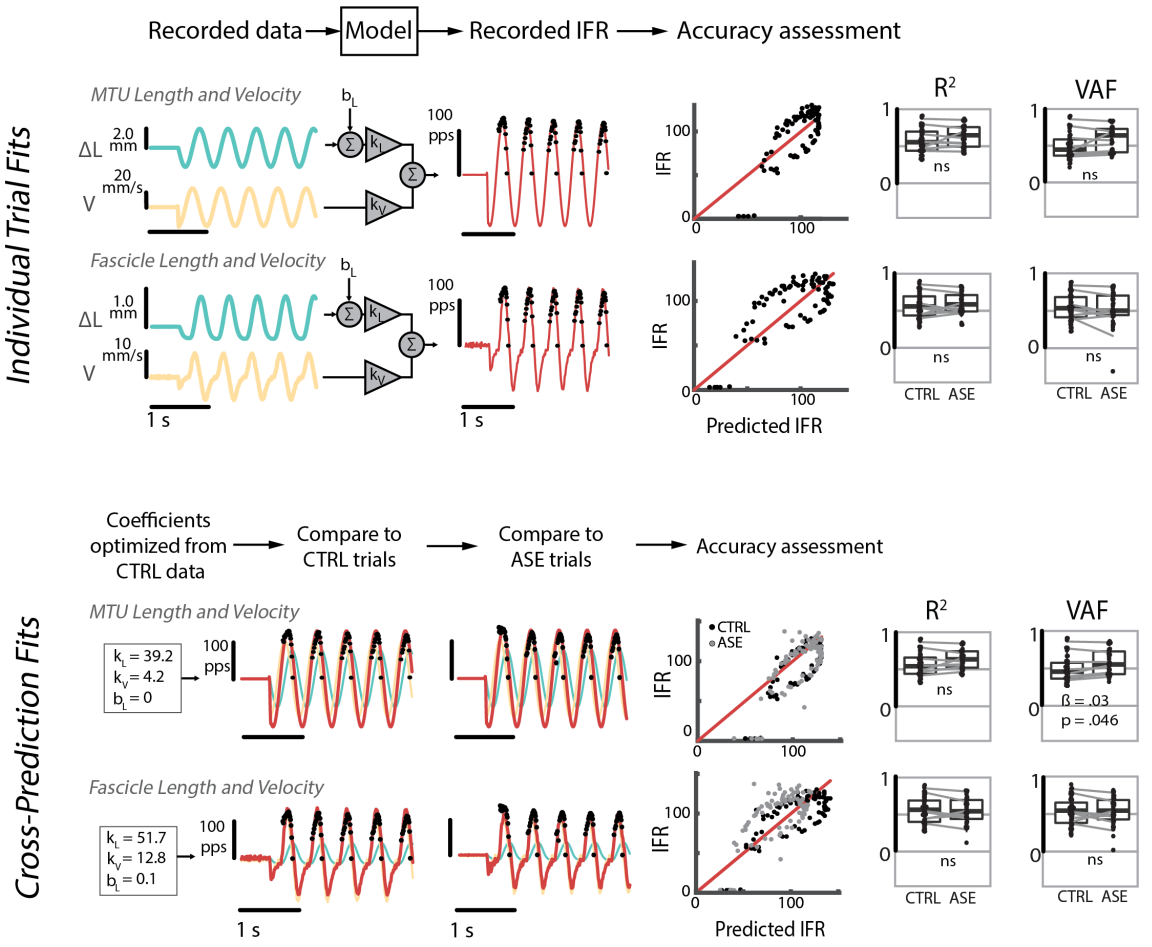

Figure 5: Predictions of muscle spindle IFR based on MTU and fascicle length and velocity. Top panel: example individual-trial fits of MTU and fascicle models. Length and velocity measurements from the MTU and fascicle are combined in a pseudo-linear manner (length component in blue, velocity component in orange) to predict spindle IFR (predictor in red, IFR black dots). Both models lack prediction accuracy in intermediate ranges of firing rates as shown in the recorded vs predicted IFR plots (right, red line indicates 1:1 relationship). Neither model suffered a loss of accuracy in ASE conditions. Bottom panel: cross-prediction fitting conducted in the same manner as in the force and yank models. Fascicle model shows a shift towards under-prediction in the ASE condition, however the only significant change in accuracy is an increase in VAF of the MTU model in the ASE condition.

Conditions, but the VAF in the ASE condition significantly increased. In the control condition, fixing coefficients resulted in no significant change in either R^2 or VAF. In the fascicle length and velocity model, no significant changes were observed in either R^2 or VAF between individual-trial fits in control and ASE conditions, fixed-coefficient fits in control and ASE conditions, or between individual-trial fits and fixed-coefficient fits in the control condition.

3.4 Nonlinear Velocity Model

The nonlinear velocity model did not accurately reproduce muscle spindle IFR. In the MTU model, firing rate was consistently over-predicted during lengthening and under-predicted during shortening, as shown in the individual fit in Fig. 6. This same behavior is apparent in the fixed-coefficient fits of the MTU model. While the fit is substantially nonlinear, there is no apparent difference in trends between control and ASE conditions. Overall, the R^2 and VAF were poor for the nonlinear MTU velocity model. Interestingly, R^2 and VAF were higher in the ASE condition in both individual-trial fits and fixed-coefficient fits for the MTU model, with no significant decrease in accuracy associated with fixing coefficients. The nonlinear fascicle velocity model produced generally better predictions of spindle firing than the accompanying MTU model. Qualitatively, the fascicle velocity measurements were able to more accurately model spindle firing during lengthening, as shown in the individual-trial and fixed-coefficient fits in Fig. 6. There was also little difference in the relationship between recorded and predicted IFR between control and ASE conditions. There were also no significant changes in R^2 or VAF between groups with individual-trial fits, fixed-coefficients fits, or between individual-trial and fixed-coefficient fits in the control condition.

Table 1: Performance metrics of force and yank, length and velocity, and nonlinear velocity models of the MTU and fascicle across conditions and fitting methods

	R^2 (mean ± sd)				VAF (mean ± sd)			
	Individual-Trial		Fixed-Coefficient		Individual-Trial		Fixed-Coefficient	
Model	(CTRL, ASE)		(CTRL, ASE)		(CTRL, ASE)		(CTRL, ASE)	
MTU Force/Yank	0.70 ± 0.14	0.71 ± 0.14	0.70 ± 0.14	0.70 ± 0.13	0.66 ± 0.14	0.71 ± 0.14	0.66 ± 0.14	0.65 ± 0.15
Fas. Force/Yank	0.71 ± 0.16	0.69 ± 0.17	0.71 ± 0.16	0.66 ± 0.18	0.64 ± 0.19	0.63 ± 0.18	0.63 ± 0.19	0.57 ± 0.22
MTU Length/Velocity	0.57 ± 0.16	0.64 ± 0.15	0.57 ± 0.16	0.64 ± 0.14	0.49 ± 0.18	0.59 ± 0.17	0.49 ± 0.17	0.59 ± 0.17
Fas. Length/Velocity	0.57 ± 0.17	0.60 ± 0.15	0.56 ± 0.18	0.56 ± 0.18	0.55 ± 0.18	0.54 ± 0.22	0.53 ± 0.18	0.54 ± 0.18
MTU Nonlinear Velocity	0.26 ± 0.09	0.31 ± 0.08	0.26 ± 0.09	0.31 ± 0.07	0.25 ± 0.09	0.30 ± 0.08	0.25 ± 0.09	0.30 ± 0.06
Fas. Nonlinear Velocity	0.53 ± 0.17	0.54 ± 0.15	0.53 ± 0.17	0.53 ± 0.16	0.52 ± 0.18	0.54 ± 0.15	0.51 ± 0.19	0.51 ± 0.18

Table 1 gives the R^2 and VAF for each model in individual fits and fixed-coefficient fits across conditions. No significant differences were observed between MTU and Fascicle force and yank models apart from in VAF in the ASE condition of individual-trial ($p < .01$, one-way repeated measures ANOVA) and fixed-coefficient ($p < .001$) fits. Of all fascicle models, force and yank performed significantly better in every metric apart from VAF in the fixed-coefficient fits in the ASE condition. Of the MTU models, force and yank performed significantly better in every metric. MTU length and velocity resulted in significantly higher R^2 in the ASE condition in both individual-trial and fixed-coefficient fits compared to fascicle length and velocity, as well as VAF in fixed-coefficient fits in the ASE condition. The fascicle length and velocity model produced higher VAF in individual-trial fits and fixed-coefficient fits in the ASE condition. The fascicle nonlinear velocity model performed significantly better than the MTU nonlinear velocity model in every metric.

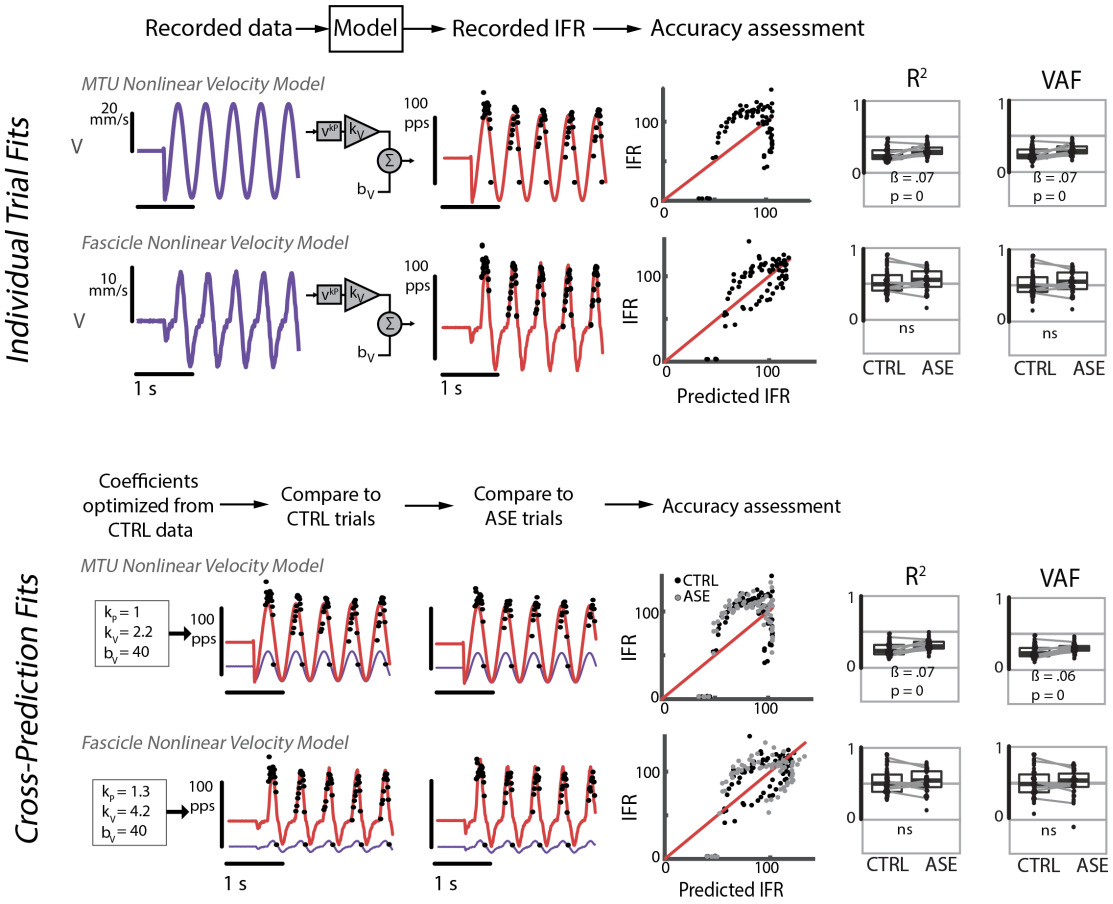

Figure 6: Predictions of muscle spindle IFR based on nonlinear MTU and fascicle velocity model. Top panel: example individual-trial fits of MTU and fascicle models. Velocity measurements from the MTU and fascicle are combined in a pseudo-linear manner with exponential gain, constant gain and constant offset to predict spindle IFR as in Prochazka and Gorassini 1998 [16]. Relationships of recorded and predicted IFR (right) show nonlinear relationships with poor accuracy (red line indicates 1:1 relationship) with improvements in prediction of the fascicle model during lengthening. Bottom panel: example trials of model fits with fixed coefficients to test cross-prediction accuracy between control and ASE conditions. Training models on control data resulted in a single set of coefficients used to predict IFR across conditions. No clear differences between recorded and predicted IFR relationships between conditions in either model.

DISCUSSION

4.1 Summary

Here, we demonstrate that tendon compliance affects sensory feedback from muscle spindles, and these changes can be accounted for by changes in forces applied to the tissue. To our knowledge, this analysis offers the first direct comparison of muscle spindle behavior with tendon compliance as an experimental factor. Additionally, while sonomicrometry has been used to describe spindle behavior in terms of local length change in previous work [10], this analysis offers a novel direct comparison of spindle firing behavior in terms of measured fascicle and MTU length changes and velocities. We also demonstrate that the experimental increase in compliance affects the relationship between muscle spindle firing and muscle fascicle length and velocity, but these differences may be accounted for by fascicle force and yank. This model also showed the most linear relationship (qualitatively) between the recorded and predicted IFR.

4.1.1 Force and Yank Model

According to our hypothesis that muscle spindles respond to the force and yank exerted on intrafusal muscle tissue, we predicted that a fascicle force and yank model would better predict muscle spindle IFR, and these predictions would be consistent across conditions. The analysis of the accuracy of the fascicle force and yank model supports this hypothesis. There was no decrease in accuracy between experimental groups with individual-trial fitting. With fixed-coefficient fitting, there was also no decrease in prediction accuracy between experimental groups, indicating that the fascicle force and

yank model predictions are generalizable across mechanical conditions. Additionally, there was no significant decrease in accuracy associated with fixing coefficients in the control condition, and one single set of coefficients could accurately represent the sensitivities of a single muscle spindle afferent across trials.

The MTU force and yank model demonstrated a similar ability to generalize across conditions. The only significant change in performance was associated with prescribing coefficients, however this change was small ($\beta = 0.003$, $p = 0.047$). Additionally, the estimated change was positive, and thus does not indicate a decrease in performance when describing the responses of the afferent with a single set of coefficients. While the fascicle force and yank model performed well, it did not offer more accurate predictions of spindle behavior than the MTU force and yank model. This may potentially be due to the experimental design and extramysial tissue force model. First, this model was developed in ramp stretches of varying amplitudes [13] which offer more qualitative information on spindle firing with which to fit the model and perhaps sinusoidal length changes alone did not offer a suitable data set with which to train the model. Second, this model was originally developed using the length of the MTU to estimate the force on extramysial tissue, while this current analysis utilized the length of the fascicle. While this may offer an advantage, it may also be possible that extramysial tissue may span the length of the MTU, and thus MTU length may offer a better model of extramysial force contribution. Additionally, forces may not be distributed evenly within the muscle fascicle, and tendons themselves exhibit hysteresis, where forces are different between lengthening and shortening phases of stretch. For these reasons, direct measurement techniques of fascicle force should be explored.

4.1.2 Length and Velocity Model

The alternative hypothesis that muscle spindles respond to the length and velocity of muscle stretch was also tested. While relationships between IFR and fascicle length and velocity were shown to be different across conditions (Fig. 3), no decrease in performance was observed between fixed-coefficient fits from control to ASE conditions in either the MTU or fascicle length and velocity models. The only significant difference in prediction accuracy was in fixed-coefficient fits between control and ASE conditions in the MTU model. Contrary to predictions, this change in accuracy was positive and no decrease in accuracy was observed. Additionally, no significant changes in accuracy were observed for the fascicle length and velocity model. Thus, the prediction that these models would result in a decrease in accuracy when generalized to the ASE condition was not confirmed.

4.1.3 Nonlinear Velocity Model

In accordance with prior work in locomotion [16], a nonlinear velocity model was also considered. Predictions of spindle behavior based on fascicle velocity were substantially more accurate than predictions based on MTU velocity, both qualitatively and quantitatively. The nonlinear fascicle velocity model resulted in more accurate predictions of spindle behavior during the lengthening phase of the stretch cycle, and predictions in both models were consistent across control and ASE conditions. Across MTU and fascicle models, the only observed changes in accuracy were increases in accuracy of the MTU model in ASE conditions in both individual-trial and fixed-coefficient fits, contrary to predictions.

4.2 Model Accuracy in a Physiological Context

These three models offer differing insights into muscle spindle behavior, but the force and yank model offers a more mechanistic explanation. While muscle spindles have been classically understood as muscle length sensors, the firing properties of muscle spindles imply a far more complex relationship to muscle mechanics than simply length and velocity, as shown in the comparisons between groups in Fig. 3. Within the encoding region of the muscle spindle, receptor currents result from deformations in the cell membrane due to local length changes. However, the strain within the encoding region is determined by the stiffness of the intrafusal muscle fibers. Thus, the firing behavior of muscle spindles can be reproduced by estimations of fascicle force [13] or by whole muscle force [12], as intrafusal muscle fibers and extrafusal muscle exhibit similar properties in the passive state [18-23]. Intrafusal fiber properties also describe the qualitative similarities between muscle spindle firing and muscle force-producing properties, such the increased response of muscle spindles that coincides with short-range stiffness in muscle fibers and rate relaxation of spindle firing that coincides with decreases in force when held at a constant length [12]. Further, a crossbridge-based model of intrafusal muscle reproduced qualitative observations of spindle behavior by estimating driving spindle currents based on the development of force within intrafusal muscle in response to imposed length changes. It has been suggested that spindles acting as force sensors would make them redundant, as Golgi tendon organs are well-described by their force-sensing properties. However, the unique firing properties and connections to the central nervous system of muscle spindles indicate that although they may also respond to force, their role is not the same as that of Golgi tendon organs. For example, the balance-correcting response associated with spindle feedback detailed by Lockhart and Ting [4] coincided with the

acceleration of the center of mass of the cat. Additionally, muscle responses during postural sway in humans have shown to occur before maximum center of mass displacement, indicating that force- and yank-sensitivity of muscle spindles, as well as the presence of initial bursts at the onset of stretch that are not observed in Golgi tendon organs, may make them well-suited for detecting the onset of perturbations and responding more rapidly than if they responded to muscle length or velocity.

Although the length and velocity and nonlinear velocity models did not produce decreases in accuracy with the addition of series elasticity, this may largely be due to the mechanical properties of the muscle. Fig. 3 shows the relationships between MTU force and estimated fascicle force with respect to fascicle length change. Both relationships are approximately linear during the lengthening phase of stretch, when spindles are the most responsive. Thus, if spindles respond to the force and yank within the muscle fascicle, during the sinusoidal stretches analysed here, it follows that length-based and velocity-based predictions of spindle firing would produce accurate estimations of spindle firing as well, both in the experiments analyzed here and in prior literature. This is also shown in the relationship of IFR to fascicle stretch in Fig. 3, where an approximately linear trend can be observed until the fascicle begins to shorten, where the effect of tendon compliance can be seen. This may also explain the observations in the nonlinear velocity models. In the control condition the stretch velocity of the fascicle with respect to the MTU was increased, and thus the MTU velocity may have failed to account for differences in MTU and fascicle dynamics. At the lower stretch lengths and velocities in the ASE condition, these relationships were more similar, and thus the nonlinear MTU velocity model was more

accurate, and the nonlinear fascicle velocity model was similarly accurate across conditions.

While an increase in effective tendon compliance served to decouple fascicle lengths and forces from those of the MTU, the decoupling effect was not sufficient to fully tease apart spindle firing from muscle mechanics. Sinusoids were utilized as they were more similar to steady-state locomotion than triangle or ramp-and-hold stretches, however Fig. 3 shows that the relationships between mechanical variables of the MTU and fascicle are still approximately linear. Prior work comparing force- and length-based models utilized the dynamic responses of spindles to ramp and triangle stretches, and sinusoidal stretches offer less information for training these models. Prior work has also shown relationships between muscle spindle initial bursts and short-range stiffness in muscle. In this current study, initial bursts and short-range stiffness were present in some trials but were not consistent across trials or afferents. It's been shown that shortening muscle fibers can eliminate short-range stiffness, so it's possible that initializing these stretches in the shortening phase resulted in some spindles losing short-range stiffness and others not due to unequal distributions of force between fascicles and fibers. It would be useful in future work to use the dynamic responses of spindles in ramp and triangle stretch paradigms to train models in conjunction with sinusoidal stretches, or to initialize sinusoids in the lengthening phase to elicit more consistent short-range stiffness from the whole muscle.

Due to the close relationships of muscle length and velocity and force and yank in passive stretches (especially sinusoidal stretches), it remains difficult to tease apart these variables. Prior work comparing force-based and length-based models relied on evoking dynamic responses from muscle spindles (initial bursts, tonic relaxation, and history

dependence), and the current experiments were designed to analyze responses during steady-state conditions. As previously mentioned, these experiments also included stretch cycles with alpha motoneuron stimulation to recruit extrafusal muscle without activating the gamma motoneurons that innervate muscle spindles. These experiments incorporating muscle activation and ASE will offer a more rigorous test of force and yank models in future work.

4.3 Congruence with Literature

Overall, this work is in agreement with prior work describing the behavior of muscle spindles with respect to MTU length, velocity, and force. Due to the relationship between imposed length changes and force on muscle fascicles, length and velocity models can suitably predict muscle spindle feedback during steady-state behaviors, as was shown here and in Prochazka and Gorassini 1998 [16]. However, in conjunction with Blum et al 2017, Blum et al 2019, and Blum et al 2020 [11-13], this work demonstrates that models of intrafusal force and yank are better predictors of muscle spindle feedback in both steady-state and dynamic stretch paradigms. Discrepancies in nonlinear velocity model accuracy from Prochazka and Gorassini 1998 [16] likely arise from differences in experimental design. The model proposed resulted in an R^2 of 0.94 for a locomotor cycle with a duration of approximately 1 s, a much slower frequency than the 2 Hz sinusoids compared here. At a slower frequency, nonlinear MTU velocity models may predict spindle firing more accurately. For individual-trial fits, the mean k_P was 0.61, compared to 0.6 in Prochazka and Gorassini 1998. The mean k_V and b_V values were 13.7 and 48.1, respectively, compared to 4.3 and 82 previously.

This current work indicates that tendon compliance affects muscle spindle feedback, contrary to the findings of Elek et al in 1990 [30]. In this prior work, MTU length and spindle responses were recorded during locomotion in cats and reproduced with imposed length changes of the MTU, following the same pattern with and without alpha and gamma motoneuron stimulation. Using spindle firing as a measurement of fascicle length change to estimate the compliance of the tendon, it was concluded that tendon compliance had little effect on the relationship of spindle firing and MTU length as fascicle and MTU length did not differ significantly between active and passive stretch cycles. This work demonstrates clear effects of tendon compliance on muscle spindle behavior, with the added benefit of directly measuring fascicle length change. The current analysis as well as the nonlinear relationship between muscle length and spindle firing described by Matthews and Stein [14] demonstrate that muscle spindle firing is not an accurate measure of fascicle stretch. Additionally, Elek et al reported no difference in spindle firing with alpha motoneuron stimulation during stretch, which is contradicted in this current study. As previously mentioned, the trials analysed here were passive cycles isolated from trials of sinusoidal stretches with alpha motoneuron stimulation, and in these trials, extrafusal muscle activation by alpha motoneuron stimulation often has a silencing effect on muscle spindles, with no firing during active lengthening. Thus, it may be that gamma motoneuron stimulation affected the responsiveness of muscle spindles during the active lengthening cycles in Elek et al 1990 [30].

4.4 Clinical Implications

It is unclear whether tendon compliance may directly affect the neural control of movement via decreased stretch responses from muscle spindles. No significant decrease in spindle firing across all afferents was observed here with the addition of series elastic elements. However, peak and mean firing rates decreased in all but one afferent, so a larger sample size may be needed to reach a conclusive answer. It has been observed in older adults that balance control shifts from more automated, subcortical mechanisms to more cortical control [31] and that a loss of muscle spindle and Golgi tendon organ feedback result in a reduction of sensorimotor activity in amputees [9], so it is plausible that sensory feedback loss may significantly affect motor control in humans. However, it is also possible that a loss of stiffness in the tendon may be accounted for by increased activation of the muscle to retain the stiffness of the MTU. It's been shown that older adults simultaneously contract slow muscle fibers in the tibialis anterior and medial gastrocnemius during standing balance tasks, a possible compensatory mechanism to retain stiffness about the ankle joint [32-34]. This may be a strategy to increase the resting stiffness about the joint by activating muscle tissue via alpha motoneurons, however the central nervous system may also be activating gamma motoneurons in tandem to simultaneously increase the responsiveness of muscle spindles. However, whether co-contraction of agonist and antagonist muscles is an effective compensation for potential sensory loss is a question that warrants further exploration.

In conjunction with prior work, this analysis demonstrates that force and yank best describe the firing behaviors of muscle spindles in both dynamic and steady-state behaviors. It has been shown previously that different contributions of force and yank to

spindle behavior can predict observed spindle responses in different neurological conditions [11], and this work shows that a force and yank model can generalize across mechanical conditions as well. With an understanding of both the mechanical and neural contributions to spindle behavior, it would then be possible to develop mechanical solutions to neurological problems. For example, a condition such as cerebral palsy that is associated with hyperactivity of stretch reflexes [26, 27, 35, 36], a mechanical intervention to dampen the force and yank experienced by the muscle has the potential to improve motor function.

CONCLUSION

In this present study, we aimed to study the effect of tendon compliance on muscle spindle feedback and test the hypothesis that muscle spindles respond to the force and yank exerted on intrafusal muscle fibers by testing mathematical models of spindle behavior in passive stretches of the rat medial gastrocnemius MTU with and without added series elasticity. We alternatively tested models of muscle spindle behavior based on measured MTU length change and velocity and fascicle length change and velocity measured via sonomicrometry. The utilization of sonomicrometry offered a novel opportunity to directly compare MTU and fascicle dynamics in a manner not previously seen in the literature. Not only did force and yank-based models accurately predict spindle IFR, but predictions also generalized across mechanical conditions with no loss in prediction accuracy, supporting the hypothesis that spindles respond to force and yank on the spindle. Length and velocity-based models equally generalized across conditions but were less accurate predictors of muscle spindle firing rate. Ultimately, this work demonstrates that tendon compliance affects sensory feedback from muscles and decouples relationships between MTU and fascicle mechanics, and in conjunction with prior work, that models of the force and yank on intrafusal muscle can accurately predict muscle spindle feedback in steady-state and dynamic conditions.

REFERENCES

[1] J. A. Vincent et al., "Muscle proprioceptors in adult rat: mechanosensory signaling and synapse distribution in spinal cord," Journal of Neurophysiology, vol. 118, no. 5, pp. 2687–2701, Nov. 2017, doi: 10.1152/jn.00497.2017.

[2] A. Takeoka, I. Vollenweider, G. Courtine, and S. Arber, "Muscle Spindle Feedback Directs Locomotor Recovery and Circuit Reorganization after Spinal Cord Injury," Cell, vol. 159, no. 7, pp. 1626–1639, Dec. 2014, doi: 10.1016/j.cell.2014.11.019.

[3] J. C. Rothwell, M. M. Traub, B. L. Day, J. A. Obeso, P. K. Thomas, and C. D. Marsden, "MANUAL MOTOR PERFORMANCE IN A DEAFFERENTED MAN," Brain, vol. 105, no. 3, pp. 515–542, 1982, doi: 10.1093/brain/105.3.515.[2] BROWN, G. L. and ROSHKO, A. "The effect of names in full upper case in numerical references," J. Fluid Mech., vol. 26, pp. 225–236, 1966.

[4] D. B. Lockhart and L. H. Ting, "Optimal sensorimotor transformations for balance," Nat. Neurosci., vol. 10, no. 10, pp. 1329–1336, Oct. 2007, doi: 10.1038/nn1986.

[5] C. F. Honeycutt, J. S. Gottschall, and T. R. Nichols, "Electromyographic responses from the hindlimb muscles of the decerebrate cat to horizontal support surface perturbations," J Neurophysiol, vol. 101, no. 6, pp. 2751–2761, Jun. 2009, doi: 10.1152/jn.91040.2008.

[6] C. F. Honeycutt, P. Nardelli, T. C. Cope, and T. R. Nichols, "Muscle spindle responses to horizontal support surface perturbation in the anesthetized cat: insights into the role of autogenic feedback in whole body postural control," J Neurophysiol, vol. 108, no. 5, pp. 1253–1261, Sep. 2012, doi: 10.1152/jn.00929.2011.

[7] T. A. Abelew, M. D. Miller, T. C. Cope, and T. R. Nichols, "Local Loss of Proprioception Results in Disruption of Interjoint Coordination During Locomotion in the Cat," Journal of Neurophysiology, vol. 84, no. 5, pp. 2709–2714, Nov. 2000, doi: 10.1152/jn.2000.84.5.2709.

[8] W. P. Mayer and T. Akay, "The Role of Muscle Spindle Feedback in the Guidance of Hindlimb Movement by the Ipsilateral Forelimb during Locomotion in Mice,"

eNeuro, vol. 8, no. 6, p. ENEURO.0432-21.2021, Dec. 2021, doi: 10.1523/ENEURO.0432-21.2021.

[9] S. S. Srinivasan et al., "Agonist-antagonist myoneural interface amputation preserves proprioceptive sensorimotor neurophysiology in lower limbs," Science Translational Medicine, vol. 12, no. 573, p. eabc5926, Dec. 2020, doi: 10.1126/scitranslmed.abc5926.

[10] J. A. Hoffer, A. A. Caputi, I. E. Pose, and R. I. Griffiths, "Chapter 7 Roles of muscle activity and load on the relationship between muscle spindle length and whole muscle length in the freely walking cat," in Progress in Brain Research, vol. 80, Elsevier, 1989, pp. 75–85. Doi: 10.1016/S0079-6123(08)62201-3.

[11] K. P. Blum et al., "Diverse muscle spindle firing properties emerge from multiscale muscle mechanics," bioRxiv, p. 858209, In Revision, doi: 10.1101/858209, eLife.

[12] K. P. Blum, B. Lamotte D'Incamps, D. Zytnicki, and L. H. Ting, "Force encoding in muscle spindles during stretch of passive muscle," PloS Comput Biol, vol. 13, no. 9, Sep. 2017, doi: 10.1371/journal.pcbi.1005767.

[13] K. P. Blum, P. Nardelli, T. C. Cope, and L. H. Ting, "Elastic tissue forces mask muscle fiber forces underlying muscle spindle Ia afferent firing rates in stretch of relaxed rat muscle," J. Exp. Biol., vol. 222, no. Pt 15, Aug. 2019, doi: 10.1242/jeb.196287.

[14] P. B. Matthews and R. B. Stein, "The sensitivity of muscle spindle afferents to small sinusoidal changes of length," J. Physiol. (Lond.), vol. 200, no. 3, pp. 723–743, Feb. 1969, doi: 10.1113/jphysiol.1969.sp008719.

[15] P. B. C. Matthews, "The response of de-efferented muscle spindle receptors to stretching at different velocities," The Journal of Physiology, vol. 168, no. 3, pp. 660–678, 1963, doi: 10.1113/jphysiol.1963.sp007214.

[16] A. Prochazka and M. Gorassini, "Ensemble firing of muscle afferents recorded during normal locomotion in cats," The Journal of Physiology, vol. 507, no. 1, pp. 293–304, Feb. 1998, doi: 10.1111/j.1469-7793.1998.293bu.x.

[17] J. Day, L. R. Bent, I. Birznieks, V. G. Macefield, and A. G. Cresswell, "Muscle spindles in human tibialis anterior encode muscle fascicle length changes," Journal

of Neurophysiology, vol. 117, no. 4, pp. 1489–1498, Apr. 2017, doi: 10.1152/jn.00374.2016.

[18] V. K. Haftel, E. K. Bichler, T. R. Nichols, M. J. Pinter, and T. C. Cope, "Movement reduces the dynamic response of muscle spindle afferents and motoneuron synaptic potentials in rat," J. Neurophysiol., vol. 91, no. 5, pp. 2164–2171, May 2004, doi: 10.1152/jn.01147.2003.

[19] U. Proske and D. L. Morgan, "Do cross-bridges contribute to the tension during stretch of passive muscle?," J. Muscle Res. Cell. Motil., vol. 20, no. 5–6, pp. 433–442, Aug. 1999, doi: 10.1023/a:1005573625675.

[20] U. Proske and G. J. Stuart, "The initial burst of impulses in responses of toad muscle spindles during stretch.," The Journal of Physiology, vol. 368, no. 1, pp. 1–17, Nov. 1985, doi: 10.1113/jphysiol.1985.sp015843.

[21] K. S. Campbell and M. Lakie, "A cross-bridge mechanism can explain the thixotropic short-range elastic component of relaxed frog skeletal muscle," J. Physiol. (Lond.), vol. 510 (Pt 3), pp. 941–962, Aug. 1998, doi: 10.1111/j.1469-7793.1998.941bj.x.

[22] K. S. Campbell and R. L. Moss, "A thixotropic effect in contracting rabbit psoas muscle: prior movement reduces the initial tension response to stretch," J. Physiol. (Lond.), vol. 525 Pt 2, no. 2, pp. 531–548, Jun. 2000, doi: 10.1111/j.1469-7793.2000.00531.x.

[23] K. S. Campbell and R. L. Moss, "History-dependent mechanical properties of permeabilized rat soleus muscle fibers," Biophys. J., vol. 82, no. 2, pp. 929–943, Feb. 2002, doi: 10.1016/S0006-3495(02)75454-4.

[24] R. B. Svensson, K. M. Heinemeier, C. Couppé, M. Kjaer, and S. P. Magnusson, "Effect of aging and exercise on the tendon," Journal of Applied Physiology, vol. 121, no. 6, pp. 1353–1362, Dec. 2016, doi: 10.1152/japplphysiol.00328.2016.

[25] J. I. Quinlan, M. V. Narici, N. D. Reeves, and M. V. Franchi, "Tendon Adaptations to Eccentric Exercise and the Implications for Older Adults," JFMK, vol. 4, no. 3, p. 60, Aug. 2019, doi: 10.3390/jfmk4030060.

[26] F. De Groote, K. P. Blum, B. C. Horslen, and L. H. Ting, "Interaction between muscle tone, short-range stiffness and increased sensory feedback gains explains key

kinematic features of the pendulum test in spastic cerebral palsy: A simulation study," PloS ONE, vol. 13, no. 10, p. e0205763, Oct. 2018, doi: 10.1371/journal.pone.0205763.

[27] A. Falisse, L. Bar-On, K. Desloovere, I. Jonkers, and F. De Groote, "A spasticity model based on feedback from muscle force explains muscle activity during passive stretches and gait in children with cerebral palsy," PloS One, vol. 13, no. 12, pp. e0208811–e0208811, Dec. 2018, doi: 10.1371/journal.pone.0208811.

[28] Correlation coefficients – MATLAB. [Online]. Available: https://www.mathworks.com/help/matlab/ref/corrcoef.html. [Accessed: 13-Jun-2022].

[29] VAF, 01-Aug-2007. [Online]. Available: https://www.mathworks.com/matlabcentral/mlc-downloads/downloads/8c84de26-d2df-4a96-8ae7-b117029c1629/6bacf814-8511-40e6-bd06-6dc3c692e8c9/previews/doc/html/vaf.html. [Accessed: 13-Jun-2022].

[30] J. Elek, A. Prochazka, M. Hulliger, and S. Vincent, "In-series compliance of gastrocnemius muscle in cat step cycle: do spindles signal origin-to-insertion length?," J. Physiol. (Lond.), vol. 429, pp. 237–258, Oct. 1990, doi: 10.1113/jphysiol.1990.sp018254.

[31] I. Melzer, N. Benjuya, and J. Kaplanski, "Age-Related Changes of Postural Control: Effect of Cognitive Tasks," Gerontology, vol. 47, no. 4, pp. 189–194, 2001, doi: 10.1159/000052797.

[32] R. V. Vitali, V. J. Barone, J. Ferris, L. A. Stirling, and K. H. Sienko, "Effects of Concurrent and Terminal Visual Feedback on Ankle Co-Contraction in Older Adults during Standing Balance," Sensors, vol. 21, no. 21, p. 7305, Nov. 2021, doi: 10.3390/s21217305.

[33] L. Alizadehsaravi, S. M. Bruijn, H. Maas, and J. H. van Dieën, "Modulation of soleus muscle H-reflexes and ankle muscle co-contraction with surface compliance during unipedal balancing in young and older adults," Exp Brain Res, vol. 238, no. 6, pp. 1371–1383, Jun. 2020, doi: 10.1007/s00221-020-05784-0.

[34] M. M. DaSilva et al., "Muscle co-contractions are greater in older adults during walking at self-selected speeds over uneven compared to even surfaces," Journal of Biomechanics, vol. 128, p. 110718, Nov. 2021, doi: 10.1016/j.jbiomech.2021.110718.

[35] A. T. Smith and M. A. Gorassini, “Hyperexcitability of brain stem pathways in cerebral palsy,” Journal of Neurophysiology, vol. 120, no. 3, pp. 1428–1437, Sep. 2018, doi: 10.1152/jn.00185.2018.

[36] E. G. Condliffe, D. T. Jeffery, D. J. Emery, and M. A. Gorassini, “Spinal inhibition and motor function in adults with spastic cerebral palsy: Spinal inhibition in adult spastic cerebral palsy,” J Physiol, vol. 594, no. 10, pp. 2691–2705, May 2016, doi: 10.1113/JP271886.